Critical analysis of topological charge determination in the background of center vortices in $SU(2)$ lattice gauge theory

R. Höllwieser,[1] M. Faber,[1] and U. M. Heller[2]

[1]*Atomic Institute, Vienna University of Technology, Wiedner Hauptstraße 8-10, A-1040 Vienna, Austria*
[2]*American Physical Society, One Research Road, Ridge, New York 11961, USA*

(Received 14 February 2012; revised manuscript received 20 May 2012; published 30 July 2012)

We analyze topological charge contributions from classical $SU(2)$ center vortices with shapes of planes and spheres using different topological charge definitions, namely the center vortex picture of topological charge, a discrete version of $F\tilde{F}$ in the plaquette or hypercube definitions and the lattice index theorem. For the latter the zero modes of the Dirac operator in the fundamental and adjoint representations using both the overlap and asqtad staggered fermion formulations are investigated. We find several problems for the individual definitions and discuss the discrepancies between the different topological charge definitions. Our results show that the interpretation of topological charge in the background of center vortices is rather subtle.

DOI: 10.1103/PhysRevD.86.014513 PACS numbers: 11.15.Ha, 12.38.Aw

I. INTRODUCTION

Since Savvidy [1] we know that the QCD vacuum is nontrivial and has magnetic properties. In lattice QCD it was shown [2] that vortices (quantized magnetic fluxes) condense in the vacuum and compress the electric flux between quark and antiquark to a string leading to confinement. This center vortex model [3–8] seems to be a very promising candidate to explain the phenomena that dominate the infrared regime. Numerical simulations have indicated that vortices could also account for phenomena related to chiral symmetry, such as causing topological charge fluctuations and spontaneous chiral symmetry breaking (SCSB) [9–12]. In particular, [13] states that the topological charge of a vortex gauge field can be determined from the shape and orientation of P vortices, i.e. from vortex intersections and writhing points.

Center vortices are based on a discrete gauge symmetry of the action. A nontrivial center transformation of all link variables in one time (or space) slice [2]

$$U_0(\vec{x}, t_0) \Rightarrow zU_0(\vec{x}, t_0), \qquad z \in Z_N \tag{1.1}$$

leaves the action invariant. More generally, this transformation can be expressed in terms of gauge transformations on a periodic lattice

$$U_0(\vec{x}, t_0) \Rightarrow g(x, t)U_0(\vec{x}, t_0)g^\dagger(x, t+1) \tag{1.2}$$

which are periodic in the time direction only up to a Z_N transformation:

$$g(\vec{x}, t_0 + L_t) = zg(\vec{x}, t_0), \qquad z \in Z_N. \tag{1.3}$$

This "singular" gauge transformation is not really a gauge transformation, since it affects of course the Polyakov loop, a gauge-invariant observable. Restricting such a transformation to a finite volume of a slice, the three dimensional Dirac volume, increases the action by a surface contribution, the vortex action. However, center vortices also increase the entropy, compensating the rise of the action and giving essential contributions to the vacuum configurations [14]. The appearance of link variables close to nontrivial center elements survives the continuum limit and leads to singular gauge fields. This implies the question of whether center vortices are lattice artifacts. One could give a positive answer, if removing such lattice artifacts would not influence QCD. But it is just the opposite: removing center vortices destroys confinement and the topological charge vanishes [9]. This means center vortices are an essential ingredient of the QCD vacuum.

II. TOPOLOGY ON THE LATTICE

In lattice calculations there is a common method to determine the topological charge Q_U from the integral

$$Q_U = -\frac{1}{16\pi^2}\int d^4x \,\mathrm{Tr}[\tilde{F}_{\mu\nu}F_{\mu\nu}], \tag{2.1}$$

where $F_{\mu\nu}$ is expressed in terms of the plaquette field

$$P_{\mu\nu} = U_\mu(x)U_\nu(x+\mu)U_\mu^\dagger(x+\nu)U_\nu^\dagger(x). \tag{2.2}$$

This expression is derived in the continuum from the transition between vacua with different winding numbers [15,16]

$$\begin{aligned} Q &= \int_{S_3} J_\mu d\sigma_\mu, \\ J_\mu &= -\frac{1}{8\pi^2}\epsilon_{\mu\nu\alpha\beta}\,\mathrm{Tr}(A_\nu\partial_\alpha A_\beta + 2/3 A_\nu A_\alpha A_\beta). \end{aligned} \tag{2.3}$$

Since $F_{\mu\nu}\tilde{F}_{\mu\nu} = \partial_\mu J_\mu$, Q can be re-expressed as the above volume integral (2.1). On the lattice, continuity in space is lost and it seems that one should be able to view any lattice field configuration as being a discrete copy of a smooth continuum configuration. This would always be topologically trivial, since $F\tilde{F}$ is a total derivative.

Nonzero Q_U may come from field configurations containing gauge singularities [17–19].

Another possibility to analyze the topology of a gauge field is given by the Atiyah-Singer index theorem [20–23]. It states that the topological charge of a gauge field configuration is proportional to the index of the Dirac operator in this gauge field background. For the overlap Dirac operator [23–25] in the fundamental representation the index is given by $\mathrm{ind}\, D[A] = n_- - n_+ = Q_D$, where n_- and n_+ are the number of left- and right-handed zero modes. The adjoint version of the index theorem reads $\mathrm{ind}\, D[A] = n_- - n_+ = 2NQ_D = 4Q_D$, where $N = 2$ is the number of colors and the additional factor 2 is due to the fact that the fermion is in a real representation; hence the spectrum of the adjoint Dirac operator iD is doubly degenerate. As described in [26] the improved staggered operator also produces eigenmodes which can clearly be identified as zero modes and all results in this paper show perfect agreement between the two fermion realizations, considering that the eigenvalues of the staggered fermion operator have a twofold degeneracy due to a global charge conjugation symmetry in $SU(2)$. We therefore have $\mathrm{ind}\, D[A] = n_- - n_+ = 2Q_D$ for fundamental and $\mathrm{ind}\, D[A] = n_- - n_+ = 8Q_D$ for adjoint (asqtad) staggered fermions. The lattice version of the index theorem is only valid as long as the gauge field is smooth enough and satisfies a so-called "admissibility" condition. It requires that the plaquette values $U_{\mu\nu}$ are bounded close to $\mathbb{1}$, the value for very smooth gauge fields. Sufficient, but not necessary bounds for the admissibility of the gauge field are $\|1 - U_{\mu\nu}\| < 1/30$ [17], or $\|1 - U_{\mu\nu}\| < [6(2 + \sqrt{(2)})] = 0.04882$ [27].

In this paper we discuss smooth lattice field configurations, which fulfill the admissibility condition and show clearly a discrepancy between the integral of $F\tilde{F}$ and the topological charge derived from the lattice index theorem. These configurations are thick, spherical vortices in $SU(2)$ lattice gauge theory. We analyze their topological charge and their zero modes. The problem seems to be related to the singular nature of vortex configurations; in fact, it is incorporated to the $SU(2)$ nature of our spherical vortex configuration. Here we analyze this problem in more detail and start with the discussion of plane vortices in different $U(1)$ subgroups of $SU(2)$.

III. PLANE CENTER VORTICES AND TOPOLOGICAL CHARGE CONTRIBUTIONS

For planar vortices parallel to two of the coordinate axes in $SU(2)$ lattice gauge theory we analyzed the location of Dirac zero modes in [28]. The vortices were defined by links varying in a $U(1)$ subgroup of $SU(2)$, defined by the Pauli matrices σ_i,

$$U_\mu = \exp(\mathrm{i}\phi\sigma_i). \tag{3.1}$$

The direction of the flux and the orientation of the vortices were determined by the gradient of the angle ϕ, which we choose as a piecewise linear function of the coordinate perpendicular to the vortex. The explicit functions for ϕ are given in Eq. (2.1) of [28]. For later use we plot in Fig. 1 the profile function ϕ and the corresponding t links rotating in z direction for a parallel xy vortex.

Upon traversing a vortex sheet, the angle ϕ increases or decreases by π within a finite thickness of the vortex. Center projection leads to a (thin) P vortex at half the thickness [29]. If we consider these thick, planar vortices intersecting orthogonally, each intersection carries a topological charge with modulus $|Q| = 1/2$, whose sign depends on the relative orientation of the vortex fluxes [30]. The plaquette definition simply discretizes the continuum (Minkowski) expression of the Pontryagin index to a lattice (Euclidean) version of the topological charge definition:

$$\begin{aligned} Q_U &= -\frac{1}{16\pi^2}\int d^4x\, \mathrm{tr}[\tilde{F}_{\mu\nu}F_{\mu\nu}] \\ &= -\frac{1}{32\pi^2}\int d^4x \epsilon_{\mu\nu\alpha\beta}\, \mathrm{tr}[F_{\alpha\beta}F_{\mu\nu}] \\ &= \frac{1}{4\pi^2}\int d^4x \vec{E}\cdot\vec{B}. \end{aligned} \tag{3.2}$$

We build xy vortices where only zt plaquettes are nontrivial, i.e. with an electric field E_z, and zt vortices bearing nontrivial xy plaquettes corresponding to a magnetic field B_z. The topological charge is then proportional to E_zB_z. If the angle ϕ for different vortex sheets rotates in the same $U(1)$ subgroup of $SU(2)$, then parallel crossings give $Q = 1/2$ and antiparallel crossings give $Q = -1/2$.

In distinction from the above described discussion in Ref. [28] we now change the $U(1)$ subgroup of $SU(2)$ in Eq. (3.1) for the two crossing vortices. The profile function ϕ remains the same as shown in Fig. 1. The explicit formula is again given by Eq. (2.1) in [28]. For an orthogonal choice of σ_i for E_z plaquettes (P_{zt}) by nontrivial U_t and

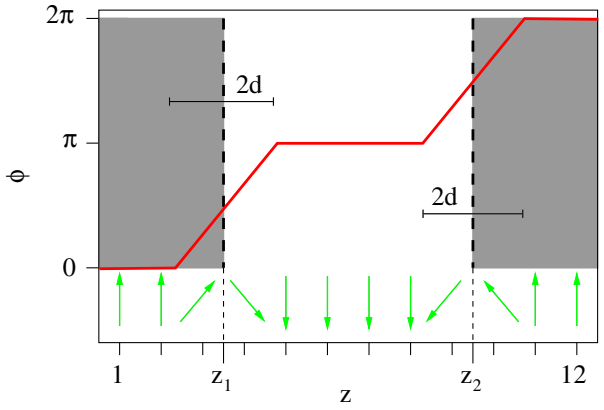

FIG. 1 (color online). The link angle ϕ of a parallel xy-vortex pair. The arrows (t links) rotate clockwise with increasing ϕ in z direction. The vertical dashed lines indicate the positions of the P vortices. In the shaded areas the links have positive (otherwise negative) trace.

$\sigma_j (i \neq j)$ for B_z plaquettes (P_{xy}) by nontrivial U_y the crossings do not contribute to the topological charge due to the orthogonality of the $U(1)$ subgroups. We note that, because the U_t and U_y links are now noncommuting, nontrivial P_{yt} plaquettes also appear in the intersection region, but nontrivial P_{xz} plaquettes are absent, since the U_x and U_z links are trivial everywhere, and so no contribution to $F\tilde{F}$ occurs. Maximal center gauge still identifies an intersecting vortex pair. But the intersection points do not carry topological charge Q_U in the $F\tilde{F}$ definition (3.2). For two intersecting vortex pairs we are able to construct configurations with topological charge $Q_U = 0, \pm 1$, and even $\pm 1/2$. The topological charge density in the intersection plane of three such configurations is shown in Figs. 2(a)–2(c). For comparison see the plots in Fig. 2 in [28]. If ϕ rotates in the σ_1 subgroup for the xy vortex and in σ_2 for the zt vortex then $F\tilde{F}$ gives no contribution to the topological charge. If we choose the first vortex sheet of the zt vortex to rotate ϕ from zero to π in σ_1 and on to 2π in σ_2 for the second vortex sheet, whereas the xy vortex only rotates in σ_1, we get topological charge $Q_U = 1$ with a distribution shown in Fig. 2(a). If we rotate ϕ for the xy vortex with the exchanged $U(1)$ subgroups as for the zt vortex from above, i.e. starting with a σ_2 rotation and rotating the second vortex sheet in σ_1 we still get $Q_U = 1$ but now distributed as shown in Fig. 2(b). Finally, if we take the zt vortex from above, i.e. σ_1 and σ_2 vortex sheets, and for the xy vortex σ_2 and σ_3 vortex sheets, we find $Q_U = 1/2$ distributed as shown in Fig. 2(c) with an action density in the intersection plane shown in Fig. 2(d).

The action density in Fig. 2(d) already shows that such orthogonal color vector intersections might be suppressed

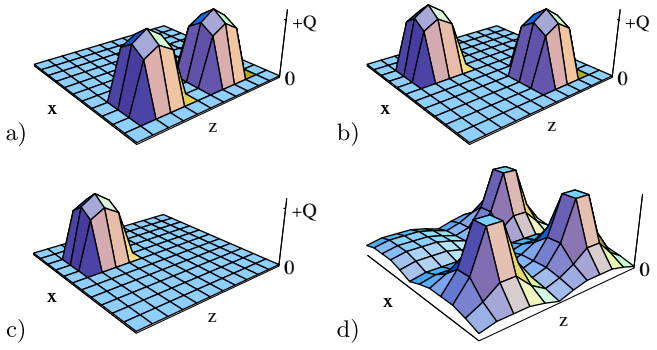

FIG. 2 (color online). Topological charge density via $F\tilde{F}$ for two parallel vortices intersecting in four points (same geometry as in Fig. 1 of [28]) in the intersection plane. In all diagrams the first sheet of the zt vortex rotates ϕ in x direction from front to back from zero to π in σ_1 and on to 2π in σ_2 for the second vortex sheet, whereas in (a) the xy vortex rotates along z from left to right in σ_1 only. In (b) the xy vortex starts with σ_2 in the first sheet and continues with σ_1. In (a) and (b) we get $Q_U = 1$. In (c) the xy vortex starts with σ_2 in the first sheet and continues with σ_3 leading to $Q_U = 1/2$. In (d) the action density in the intersection plane is shown for configuration (c).

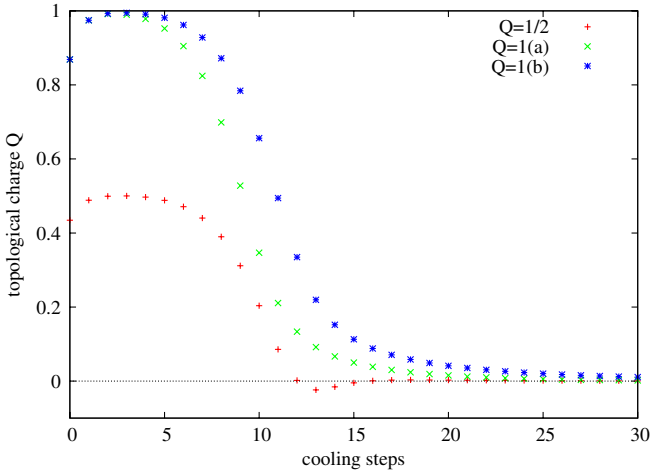

FIG. 3 (color online). Topological charge during cooling the (metastable) $Q = 1$ and $Q = 1/2$ configurations of Fig. 2. The intersecting vortex sheets end up with antiparallel orientation and the topological charge vanishes.

due to higher action and in fact, at the intersection points we find maximally nontrivial (yt) plaquettes

$$P_{yt} \approx (-i\sigma_k)(-i\sigma_l) i\sigma_k i\sigma_l = (\sigma_k\sigma_l)(\sigma_k\sigma_l) = i\sigma_m i\sigma_m = -\mathbb{1}. \quad (3.3)$$

These rough configurations also seem to trouble the Dirac operators, which do not find any zero modes. During cooling the $Q_U = 1$ and $Q_U = 1/2$ configurations of Fig. 2 are only metastable and soon turn to antiparallel vortex pairs with vanishing topological charge (see Fig. 3), whereas an original $Q_U = 0$ configuration from two parallel vortex pairs in different $U(1)$ subgroups prefers the $S = 2S_{\text{inst}}$ action minimum and ends up with parallel color vectors yielding $Q_U = 2$ (see Fig. 4). For admissible gauge

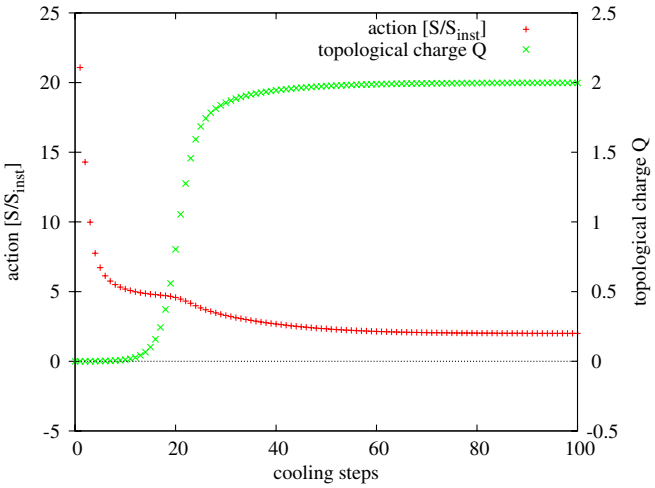

FIG. 4 (color online). During cooling the $Q = 0$ configuration, the action reaches a plateau with $S = 2S_{\text{inst}}$ and the parallel vortex pairs end up with parallel color vectors equivalent to the $Q = 2$ configuration.

fields (after some cooling) we also find the corresponding numbers of zero modes, i.e. the different definitions of topological charge agree with each other ($Q_U = Q_D$).

Nevertheless, in the next section we discuss a lattice configuration which immediately guarantees the admissibility condition but gives a discrepancy ($Q_U \neq Q_D$).

IV. THE "SPHERICAL VORTEX PROBLEM"

The spherical vortex of radius R and thickness Δ was introduced in [31] and analyzed in more detail in [26]. It is constructed with the following links:

$$U_\mu(x_\nu) = \begin{cases} \exp(i\alpha(|\vec{r} - \vec{r}_0|)\vec{n} \cdot \vec{\sigma}) & t = 1, \mu = 4 \\ \mathbb{1} & \text{elsewhere} \end{cases} \quad (4.1)$$

$$\text{with} \quad \vec{n}(\vec{r}, t) = \frac{\vec{r} - \vec{r}_0}{|\vec{r} - \vec{r}_0|}, \quad (4.2)$$

where $\vec{r}$ is the spatial part of x_ν and the profile function α is either one of α_+, α_-, which are defined by

$$\alpha_+(r) = \begin{cases} 0 & r < R - \frac{\Delta}{2} \\ \frac{\pi}{2}\left(1 + \frac{r-R}{\frac{\Delta}{2}}\right) & R - \frac{\Delta}{2} < r < R + \frac{\Delta}{2} \\ \pi & R + \frac{\Delta}{2} < r, \end{cases} \quad (4.3)$$

$$\alpha_-(r) = \begin{cases} \pi & r < R - \frac{\Delta}{2} \\ \frac{\pi}{2}\left(1 - \frac{r-R}{\frac{\Delta}{2}}\right) & R - \frac{\Delta}{2} < r < R + \frac{\Delta}{2} \\ 0 & R + \frac{\Delta}{2} < r. \end{cases} \quad (4.4)$$

This means that all links are equal to $\mathbb{1}$ except for the t links in a single time slice at fixed $t = 1$. The phase changes from 0 to π from inside to outside for $\alpha_+(r)$ [or vice versa for $\alpha_-(r)$]. The graph of $\alpha_-(r)$ is plotted in Fig. 2 in [31], giving a hedgehoglike configuration, since the color vector $\vec{n}$ points in the "radial" direction $\vec{r}/r$ at the vortex radius R. The hedgehoglike structure is crucial for our analysis, leading to the mentioned discrepancy. In maximal center gauge and after center projection, this configuration shows a single, spherical vortex without any intersection or writhing points and hence no topological charge. It is of course possible to construct the same thin spherical vortex after center projection without the hedgehog structure, simply by replacing $\vec{n}\,\vec{\sigma}$ by e.g. σ_3. Such a vortex has a smooth transition, i.e., it is homotopic, to a trivial gauge field. But as in the previous section we are interested in the analysis of topological charge behavior for colorful vortices.

We would like to underline that for the spherical vortex with the hedgehog structure there is nowhere a discontinuity in the link variables, not in the center of the three-dimensional spherical vortex nor at the lattice boundary. In both regions the link variables are center elements as necessary for a center vortex. In spite of the hedgehog structure at the two-dimensional center projected vortex sphere there is no singularity due to the full covering of S^3 by the link variables. In other words one can explain the configuration with t links of one time slice rotating from the "south pole" $-\mathbb{1}$ to the "north pole" $+\mathbb{1}$ of S^3 in radial direction from the center to the boundary, via color vectors $\vec{n}\,\vec{\sigma}$ given by the spatial components $\vec{n} = \vec{r}/r$ of the radius vector. Hence, at the center of the vortex sphere the links belong to the south pole of S^3, at the two-dimensional vortex surface to the "equator" and at the boundary of the time slice to the north pole of S^3. In other words, the links $U_t(x, y, z)$ define a smooth nontrivial mapping of $S_3 \cong SU(2)$ to $R_3 \cup \infty \cong S_3$ which does not contain any singularity. The only singularity that remains in this configuration is the singular gauge transformation leading to the vortex, but such singular gauge transformations are crucial for any vortex structure, as discussed in the introduction.

Now, since only links in the time direction are different from $\mathbb{1}$ for this spherical vortex configuration, the topological charge Q_U determined from any lattice version of $F\tilde{F}$ vanishes for this spherical vortex configuration. The index of the considered Dirac operators however is nonzero, resulting in $Q_D = \mp 1$, for $\alpha_\pm$. On a $136^3 \times N_t$ lattice the plaquettes for the spherical vortex, Eq. (4.1), satisfy the admissibility condition. In fact, the plaquettes get smaller and smaller the bigger the lattice, if we choose R and Δ to be proportional to the lattice size. We can even get rid of negative links with proper gauges (Landau gauge), ending up in a lattice gauge field with no sign of hiding a singularity at all.

In order to understand the discrepancy we apply standard cooling to the spherical vortex configuration. For many cooling steps, the index of the Dirac operator does not change, but the topological charge quickly rises close to $Q_U = \mp 1$ for $\alpha_\pm$ while the action S reaches a (nonzero) plateau. So, the index of the overlap Dirac operator agrees with the topological charge via $F\tilde{F}$ ($Q_U = Q_D$) after some cooling. In Fig. 5 we plot the cooling history for a spherical vortex on a 40^4 lattice. For comparison we also plot the topological charge of an instanton during cooling, which looks pretty much the same as for the spherical vortex. In fact, the action and topological charge densities spread over more and more time-slices, developing a hyper-spherical distribution like standard instantons. We conclude that our spherical vortex develops an instanton-like structure during cooling, in agreement with [32], stating that the Hausdorff dimension of regions where the topological charge is localized tends towards the total space dimensions.

However, the vortex structure of our initial configuration is removed after a few cooling steps, i.e. the spherical vortex shrinks very quickly. This is in agreement with the fact that the vortex content of a single instanton is shrunk to a point at the center of the instanton [33,34], but it clearly shows that cooling significantly changes the content of the

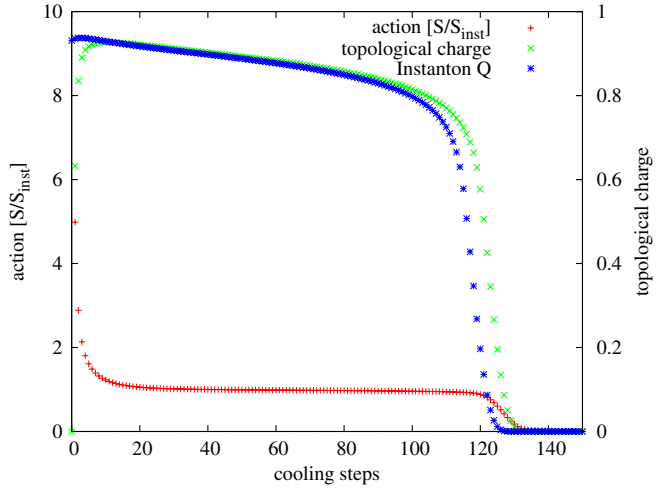

FIG. 5 (color online). Cooling of a spherical vortex on a 40^4 lattice. The topological charge rises from 0 to close to 1 for $\alpha = \alpha_-$ (right scale) while the action S (in units of the one-instanton action S_{inst}) reaches a plateau (left scale). For comparison we also plot the topological charge during cooling of an instanton.

initial gauge configuration. In Fig. 5 of [26] we showed plots of the shrinking spherical vortex and the corresponding monopole loop in Fig. 6, as well as the distribution of the scalar density of the zero modes (Fig. 3), with maxima at the inside (for α_+) or the outside (for α_-) of the vortex. In [28] we concluded that Dirac modes are sensitive to Polyakov lines, avoiding negative Polyakov lines (corresponding to negative links in the construction in [28]). Here, we add some plots of the development of topological charge density via $F\tilde{F}$ during cooling in Fig. 6, in order to show that there are no contributions from any hidden singularities. The topological charge clearly develops from the vortex surface [ring structure in Fig. 6(b)] shrinking to the center and developing an instantonlike distribution.

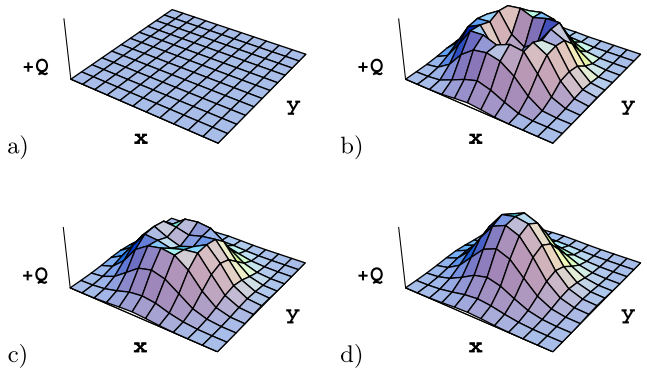

FIG. 6 (color online). Topological charge density via $F\tilde{F}$ at the xy plane through the center of the spherical vortex during cooling. Before cooling the topological charge $Q_U = 0$ (a), evolving a ring (spherical) distribution along the vortex structure after two cooling steps (b) and developing into an instantonlike (hyperspherical) distribution after 5 (c) and 10 (d) cooling steps.

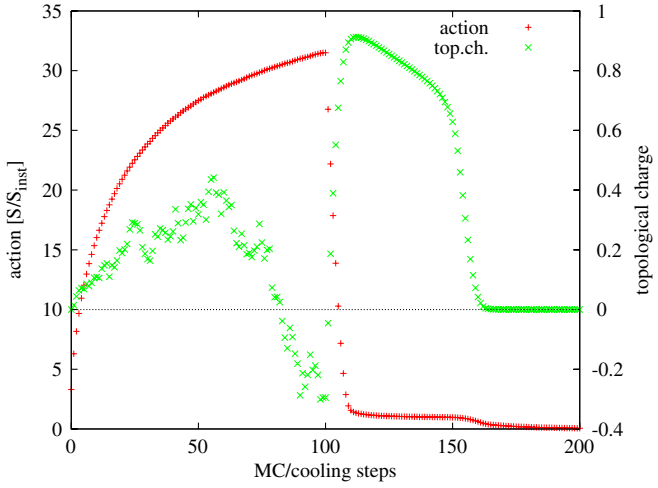

FIG. 7 (color online). Monte Carlo (Metropolis) update and cooling of a spherical vortex on a 16^4 lattice. After 100 MC steps, only after some cooling $F\tilde{F}$ reveals the same topological charge $Q_U = Q_D$ as the Dirac operator.

Further we apply some Monte Carlo steps to the spherical vortex configuration using the Metropolis algorithm with a small spread, i.e. adding small quantum fluctuations, and analyze the vortex structure and topological charge. Figure 7 shows the action and topological charge during 100 Metropolis and another 100 cooling steps. The action rises during the Monte Carlo update and the spherical vortex percolates over the whole lattice while the topological charge fluctuates around 0. The index of the lattice Dirac operator however indicates topological charge $Q_D = \mp 1$ for $\alpha_\pm$. Cooling after the Monte Carlo update

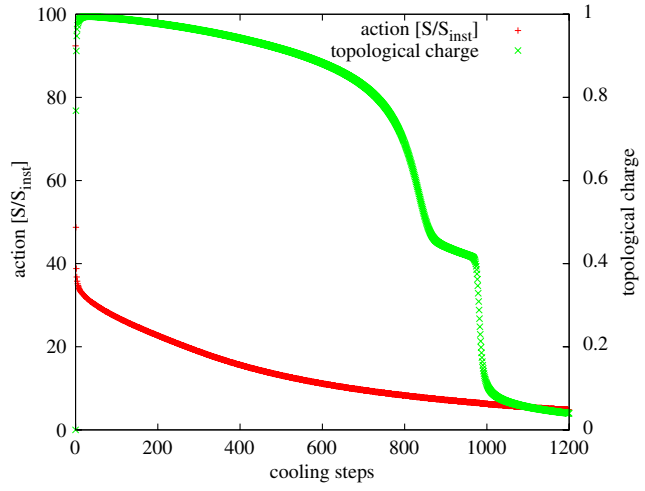

FIG. 8 (color online). Cooling of a spherical vortex on a $136^3 \times 2$ lattice. The topological charge definition $F\tilde{F}$ initially gives $Q_U = 0$, in discrepancy with the index of the Dirac operator. During cooling it rises close to 1 for $\alpha = \alpha_-$. The second plateau around 900 cooling steps indicates the fractional topological charge of a Dirac monopole; for more details see [26].

still reveals the same result for $Q_U = Q_D$ via $F\tilde{F}$, showing the same behavior as in Fig. 5.

We also want to emphasize the difference to the spherical vortex on an asymmetric lattice with time extent $N_t = 2$, which we analyzed in the second part of [26]. The vortex structure in one of the two time slices survives much longer during cooling and leads to a static, singular Dirac monopole before falling through the lattice. For completeness we also plot the cooling history of a spherical vortex on a $136^3 \times 2$ lattice in Fig. 8. The configuration initially satisfies the admissibility condition, but still shows the discrepancy between $F\tilde{F}$ and the index of the Dirac operator. The second plateau around 900 cooling steps indicates the fractional topological charge of the Dirac monopole, appearing only on the asymmetric lattice. On a symmetric lattice, we find a continuous transition to an instantonlike structure, and the vortex structure is lost. The singular gauge transformation is smoothed out in time direction at the cost of losing the center vortex.

V. DISCUSSION

We finally want to resolve the problem of topological charge determination via $F\tilde{F}$ for the above discussed spherical vortex configuration. The usual expression of topological charge Q_U (2.1) does not take into account the periodic boundary conditions of the lattice, which lead to a different topological classification, even in the large volume limit [35]. The full expression for Q must contain possible twists in the boundary conditions allowed in the adjoint representation [36–38]. However, such boundary twists may also be hidden in gauge singularities, especially in singular gauge transformations defining center vortices on the lattice. Usually one tries to evaluate the integrals for gauge invariant quantities like (2.1) in the axial gauge $A_0 = 0$, where the singularities are transformed away [39]. However, in our particular case of the spherical vortex there is no way to gauge-transform the singularity away, except by applying the inverse of the initial singular gauge transformation, which then would define the boundary twist, giving the only contribution to the topological charge of our trivial gauge field in $A_0 = 0$ gauge.

An easy way of thinking about how to determine the topological charge of a gauge field configuration is given in [18]. Woit suggests locating the gauge singularities, locally gauge-transforming them away using different gauges, and measuring the degrees of the maps relating the different gauges. The sum of these degrees will be a topological invariant, the topological charge. For our configuration we easily may follow the instructions in the above reference by splitting the lattice into time slices. We now can only consider the time slice containing our spherical vortex, where the singular gauge transformation now defines the corresponding mapping and its degree the correct topological charge.

To state the solution of our problem in a mathematical manner, we consider the homotopy of the above spherical vortex configuration, Eq. (4.1). The t links of these spherical vortices fix the holonomy of the timelike loops, defining a map $U_t(\vec{x}, t = 1)$ from the xyz hyperplane at $t = 1$ to $SU(2)$. Because of the periodic boundary conditions, the time slice has the topology of a 3-torus. But, actually, we can identify all points in the exterior of the three-dimensional sphere since the links there are trivial. Thus the topology of the time slice is $\mathbb{R}^3 \cup \{\infty\}$ which is homeomorphic to S^3. A map $S^3 \to SU(2)$ is characterized by a winding number

$$N = -\frac{1}{24\pi^2} \int d^3x \epsilon_{ijk} \mathrm{Tr}[(U^\dagger \partial_i U)(U^\dagger \partial_j U)(U^\dagger \partial_k U)],$$

resulting in $N = -1$ for positive and $N = +1$ for negative spherical vortices. With this assignment the index of the Dirac operator and the topological charge after cooling coincide with this winding number N. Obviously such windings, given by the holonomy of the timelike loops of the spherical vortex, influence the index theorem [40,41], which gives the correct definition of topological charge.

Other, topologically motivated lattice constructions of Q from the gauge field are given in [17,42], where one compares the gauge rotations necessary in contiguous cells (hypercubes) to put each cell into the same (e.g. axial) gauge. This enables one to construct transition matrices $v_{n,\mu}$ at the lattice sites n common to neighboring cells $c(n)$ and $c(n + \hat{\mu})$ which can be used to derive a geometric definition of topological charge

$$\begin{aligned} Q = -\frac{1}{24\pi^2} \sum_{n\in\Lambda} \sum_{\mu,\nu,\rho,\sigma} \epsilon_{\mu\nu\rho\sigma} \\ \times \Big\{ 3 \int_{p(n,\mu,\nu)} d^2x \, \mathrm{Tr}[(v_{n,\mu} \partial_\rho v_{n\mu}^{-1})(v_{n-\hat{\mu},\nu}^{-1} \partial_\sigma v_{n-\hat{\mu},\nu})] \\ + \int_{f(n,\mu)} d^3x \, \mathrm{Tr}[(v_{n,\mu}^{-1} \partial_\nu v_{n,\mu})(v_{n,\mu}^{-1} \partial_\rho v_{n,\mu}) \\ \times (v_{n,\mu}^{-1} \partial_\sigma v_{n,\mu})] \Big\}, \end{aligned}$$

where Λ denotes the lattice, $p(n, \mu, \nu)$ the plaquettes and $f(n, \mu)$ the faces (cubes) of a cell $c(n)$. Evaluating this expression for our spherical vortex, the only nontrivial contribution is given by the second term for $f(n, \mu = 4)$ in the time slice of our vortex, resulting in the expression for the winding number given above. All other terms vanish because of trivial transition functions or the vanishing of $F\tilde{F}$ for our configuration.

VI. CONCLUSIONS

We reported on problems defining topological charge in the background of classical center vortices on the lattice. First, planar vortex sheets are constructed by $U(1)$ rotations in a way that they intersect orthogonally. If the gauge rotations are defined in different $U(1)$ subgroups of $SU(2)$, thus defining a genuinely non-Abelian configuration, topological charge contributions at intersection points can occur which are different from the $Q = \pm 1/2$ known

to arise in Abelian vortex configurations. The use of the Dirac operator is not safe in this case because of maximally nontrivial plaquettes, which seem to suppress such configurations in the functional integral. However, for admissible gauge configurations of classical, spherical center vortices we find a discrepancy between $F\tilde{F}$ and the lattice index theorem, for both overlap and asqtad staggered fermions in the fundamental and adjoint representations. Numerically, the discrepancy equals the winding number of the spheres when they are regarded as maps $S^3 \to SU(2)$. The problem arises due to the periodic boundary conditions on the lattice and the fact that the center vortex configuration under consideration is based on a singular gauge transformation. In our case we can regard the singular gauge transformation resulting in our spherical vortex as a boundary twist, leading to an extra contribution to $F\tilde{F}$, resolving the discrepancy. However, this result shows that the interpretation of topological charge via $F\tilde{F}$ is rather subtle in the background of center vortices. The mentioned admissibility conditions do not guarantee that a naive plaquette or hypercube definition of topological charge gives a result which accords with a counting of Dirac zero modes. This is only guaranteed in the continuum limit, where vortex configurations may become singular and validate the derivation of topological charge via $F\tilde{F}$. On lattice configurations the $F\tilde{F}$ definition of topological charge should only be used after cooling, which however may change the gauge field content significantly.

ACKNOWLEDGMENTS

We are grateful to Martin Lüscher, Štefan Olejník and Mithat Ünsal for helpful discussions. This research was partially supported by the Austrian Science Fund (''Fonds zur Förderung der Wissenschaften,'' FWF) under Contract No. P22270-N16 (R. H.).

[1] G. K. Savvidy, Phys. Lett. **71B**, 133 (1977).
[2] J. Greensite, Prog. Part. Nucl. Phys. **51**, 1 (2003).
[3] G. 't Hooft, Nucl. Phys. **B138**, 1 (1978).
[4] P. Vinciarelli, Phys. Lett. **78B**, 485 (1978).
[5] T. Yoneya, Nucl. Phys. **B144**, 195 (1978).
[6] J. M. Cornwall, Nucl. Phys. **B157**, 392 (1979).
[7] G. Mack and V. B. Petkova, Ann. Phys. (N.Y.) **123**, 442 (1979).
[8] H. B. Nielsen and P. Olesen, Nucl. Phys. **B160**, 380 (1979).
[9] P. de Forcrand and M. D'Elia, Phys. Rev. Lett. **82**, 4582 (1999).
[10] C. Alexandrou, P. de Forcrand, and M. D'Elia, Nucl. Phys. **A663**, 1031c (2000).
[11] Michael Engelhardt, Nucl. Phys. **B638**, 81 (2002).
[12] M. Faber, J. Greensite, U. M. Heller, R. Höllwieser, and Š. Olejník, Phys. Rev. D **78**, 054508 (2008).
[13] H. Reinhardt and M. Engelhardt, in *Quark Confinement and the Hadron Spectrum IV*, edited by W. Lucha and K. Maung (World Scientific, Singapore, 2002), p. 150.
[14] F. V. Gubarev, A. V. Kovalenko, M. I. Polikarpov, S. N. Syritsyn, and V. I. Zakharov, Phys. Lett. B **574**, 136 (2003).
[15] A. A. Belavin, A. M. Polyakov, A. S. Schwartz, and Yu. S. Tyupkin, Phys. Lett. **59B**, 85 (1975).
[16] M. E. Peskin, Ph.D. thesis, Cornell University, 1978.
[17] M. Luscher, Commun. Math. Phys. **85**, 39 (1982).
[18] P. Woit, Phys. Rev. Lett. **51**, 638 (1983).
[19] I. A. Fox, J. P. Gilchrist, M. L. Laursen, and G. Schierholz, Phys. Rev. Lett. **54**, 749 (1985).
[20] M. F. Atiyah and I. M. Singer, Ann. Math. **93**, 139 (1971).
[21] A. S. Schwarz, Phys. Lett. **67B**, 172 (1977).
[22] L. S. Brown, R. D. Carlitz, and C.-K. Lee, Phys. Rev. D **16**, 417 (1977).
[23] R. Narayanan and H. Neuberger, Nucl. Phys. **B443**, 305 (1995).
[24] H. Neuberger, Phys. Lett. B **417**, 141 (1998).
[25] H. Neuberger, Phys. Lett. B **427**, 353 (1998).
[26] R. Höllwieser, M. Faber, and U. M. Heller, arXiv:1005.1015.
[27] H. Neuberger, Phys. Rev. D **61**, 085015 (2000).
[28] R. Höllwieser, M. Faber, and U. M. Heller, J. High Energy Phys. 06 (2011) 052.
[29] L. Del Debbio, M. Faber, J. Greensite, and Š. Olejník, Phys. Rev. D **55**, 2298 (1997).
[30] M. Engelhardt and H. Reinhardt, Nucl. Phys. **B567**, 249 (2000).
[31] G. Jordan, R. Höllwieser, M. Faber, and U. M. Heller, Phys. Rev. D **77**, 014515 (2008).
[32] P. V. Buividovich, T. Kalaydzhyan, and M. I. Polikarpov, arXiv:1111.6733.
[33] H. Reinhardt and T. Tok, Phys. Lett. B **505**, 131 (2001).
[34] F. Bruckmann and M. Engelhardt, Phys. Rev. D **68**, 105011 (2003).
[35] J. C. Wrigley, Phys. Lett. B **131**, 407 (1983).
[36] G. 't Hooft, Nucl. Phys. **B153**, 141 (1979).
[37] G. 't Hooft, Commun. Math. Phys. **81**, 267 (1981).
[38] P. van Baal, Commun. Math. Phys. **85**, 529 (1982).
[39] J. Polonyi, Phys. Rev. D **29**, 716 (1984).
[40] T. M. W. Nye and M. A. Singer, arXiv:math/0009144.
[41] E. Poppitz and M. Unsal, J. High Energy Phys. 03 (2009) 027.
[42] M. Gockeler, M. L. Laursen, G. Schierholz, and U. J. Wiese, Commun. Math. Phys. **107**, 467 (1986).